

1 A locus conferring tolerance to *Theileria* infection in African cattle

2 D. Wragg^{1,2§}, E.A.J. Cook^{3,4§}, P. Latre de Late^{3,4}, T. Sitt⁴, J.D. Hemmink^{1,3,3,4}, M. Chepkowny⁴, R. Njeru^{3,4}, E.J.
3 Poole⁴, J. Powell², E. Paxton², R. Callaby^{2,5}, A. Talenti², A.A. Miyunga^{3,4}, G. Ndambuki^{3,4}, S. Mwaura⁴, H.
4 Auty⁶, O. Matika², M. Hassan^{1,2}, K. Marshall^{3,4}, T. Connelley^{1,2}, L.J. Morrison^{1,2}, B.M.deC. Bronsvoort^{1,2}, W.I.
5 Morrison^{1,2}, P.G. Toye^{3,4†*}, J.G.D. Prendergast^{1,2†*}

6 ¹ Centre for Tropical Livestock Genetics and Health (CTLGH), Easter Bush Campus, EH25 9RG, UK

7 ² The Roslin Institute, University of Edinburgh, UK

8 ³ Centre for Tropical Livestock Genetics and Health (CTLGH), ILRI Kenya, P.O. Box 30709, Nairobi 00100,
9 Kenya

10 ⁴ ILRI Kenya, P.O. Box 30709, Nairobi 00100, Kenya

11 ⁵ The Epidemiology, Economics and Risk Assessment (EEA) Group, Easter Bush Campus, EH25 9RG, UK

12 ⁶ Institute of Biodiversity Animal Health & Comparative Medicine, College of Medical, Veterinary & Life
13 Sciences, University of Glasgow, Glasgow, G12 8QQ

14 [§] David Wragg and Elizabeth Cook contributed equally to this work

15 [†] Philip Toye and James Prendergast contributed equally to this work

16 ^{*} Corresponding authors: James G.D. Prendergast james.prendergast@roslin.ed.ac.uk

17 Philip Toye p.toye@cgiar.org

18 Abstract

19 East Coast fever, a tick-borne cattle disease caused by the *Theileria parva* parasite, is among the biggest
20 natural killers of cattle in East Africa, leading to over 1 million deaths annually. Here we report on the
21 genetic analysis of a cohort of Boran cattle demonstrating heritable tolerance to infection by *T. parva* ($h^2 =$
22 0.65, s.e. 0.57). Through a linkage analysis we identify a 6 Mb genomic region on *Bos taurus* chromosome
23 15 that is significantly associated with survival outcome following *T. parva* exposure. Testing this locus in an
24 independent cohort of animals replicates this association with survival following *T. parva* infection. A stop
25 gained polymorphism in this region was found to be highly associated with survival across both related and
26 unrelated animals, with only one of the 20 homozygote carriers (T/T) of this change succumbing to the
27 disease in contrast to 44 out of 97 animals homozygote for the reference allele (C/C). Consequently, we
28 present a genetic locus linked to tolerance of one of Africa's most important cattle diseases, raising the
29 promise of marker-assisted selection for cattle that are less susceptible to infection by *T. parva*.

30 Author Summary

31 More than a million cattle die of East Coast fever in Africa each year, the impact of which disproportionately
32 falls onto low-income, smallholder farmers. The lack of a widely accessible vaccine, heavy reliance on
33 chemicals to control the tick vector and inadequate drug treatments means that new approaches for
34 controlling the disease are urgently required. Through a genetic study of an extended pedigree of Boran
35 cattle that are more than three times less likely to succumb to the disease than matched controls, we identify
36 a region on chromosome 15 of the cattle genome associated with a high level of tolerance to the disease. We
37 show that a variant in this region is also associated with survival in an independent cohort, and is linked to
38 rates of cell expansion during infection. This genetic variant can therefore support marker-assisted selection,
39 allowing farmers to breed tolerant cattle and offers a route to introduce this beneficial DNA to non-native
40 breeds, enabling reduced disease incidence and increased productivity, which would be of benefit to millions
41 of rural smallholder farmers across Africa.

42 Introduction

43 East Coast fever (ECF), a tick-borne lymphoproliferative disease caused by the protozoan parasite *Theileria*
44 *parva*, is among the biggest natural causes of death in cattle across eastern, central and southern Africa, and
45 is estimated to be responsible for at least 1.1 million deaths per year [1]. Direct economic losses attributed to
46 deaths from ECF have been estimated at ~ US\$600 million annually [2,3], and disproportionately affect
47 small-scale low-income households [4]. The potential of *T. parva* to extend its range beyond current areas is
48 likely to increase in the next 100 years due to climate change, as conditions become more favourable for its
49 vector, the brown ear tick *Rhipicephalus appendiculatus* [5]. Cattle breeds not native to East Africa are
50 highly susceptible to ECF, and mortality rates can exceed 95% [6]. The disease is consequently a major
51 barrier to the wider introduction of productive European cattle breeds into large parts of Africa. However, as
52 ECF has exerted an unusually strong selective pressure on East African cattle since their introduction to the
53 region approximately 5000 years ago [7], various local cattle breeds have developed high levels of heritable
54 tolerance to the disease [8,9].

55 As early as the 1950s, the innate genetic tolerance of *Bos indicus* zebu cattle from ECF-endemic areas of
56 Kenya had been experimentally characterised. In 1953, Barnett [9] transported zebu from ECF-endemic and
57 non-endemic areas of Kenya to a farm free of ECF. Calves subsequently born to these animals were then
58 each exposed to a single *T. parva* infected tick. The offspring of zebu from endemic and non-endemic areas
59 of Kenya showed substantial differences in their ability to survive this infection. Colostral immunity was not
60 the cause, with subsequent studies also suggesting that colostral immunity plays little to no role in inherited
61 tolerance to ECF [10]. More recently in 2005, offspring of East African Shorthorn Zebu (EASZ) originating
62 from endemic areas of Kenya, that were born in a non-endemic area and therefore previously uninfected,
63 showed a significantly higher tolerance to challenge with a *T. parva* stabilate than not only Friesian and
64 Boran cattle, but also EASZ originating from non-endemic areas [8]. Whereas all of the EASZ from the
65 ECF-endemic area of Kenya survived infection, only 60-70% of animals from nearby ECF-non-endemic
66 areas survived the same challenge. These studies highlight that among cattle breeds there is a marked
67 difference in tolerance to infection with *T. parva*, suggesting the frequency of natural tolerance alleles differs
68 between cattle derived from ECF-endemic and ECF-non-endemic areas.

69 Despite this clear evidence for genetic tolerance among certain local breeds, there has been little work to
70 map the genetic loci driving such tolerance. In this study, we analysed an extended Boran pedigree, the
71 members of which display markedly higher tolerance to *T. parva* infection than other cattle of the same
72 breed. Through a linkage study, we identify a genomic region significantly associated with this increased
73 tolerance.

74 **Results**

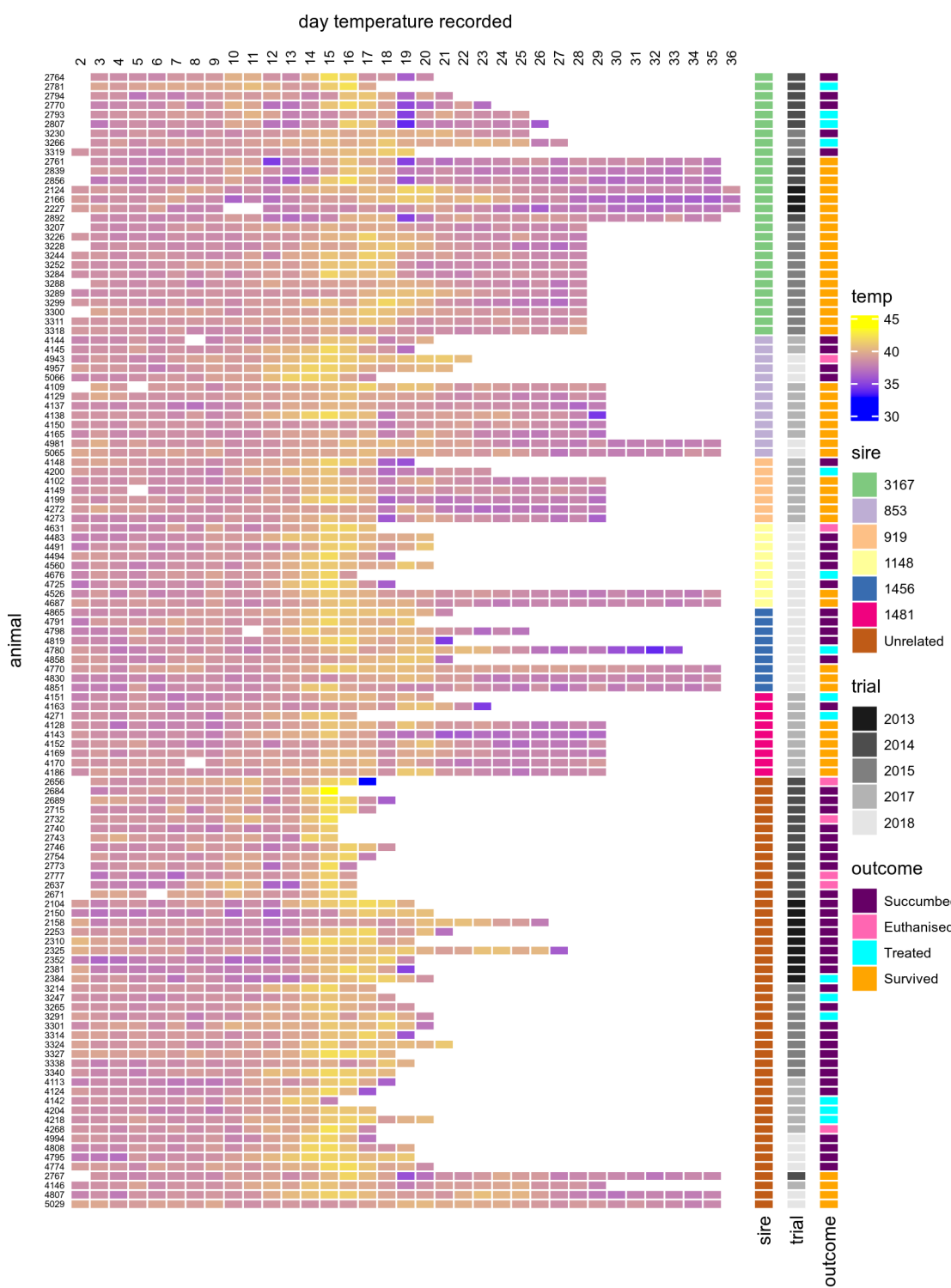
75 **Tolerance to infection by *Theileria parva* in a *Bos indicus* pedigree**

76 The initial indication of tolerance among related Boran animals was detected in a vaccine trial undertaken in
77 2013 [11], in which four out of six animals that did not succumb to infection by *T. parva* were observed to be
78 first generation descendants of the same Boran bull (3167). This included all of the three unvaccinated
79 survivors in this study. This trial was followed by two further natural field challenge trials in 2014 and 2015
80 using unvaccinated 1st generation progeny of the same sire alongside unrelated animals, and two subsequent
81 natural field challenge trials in 2017 and 2018 examining 2nd generation offspring (the progeny of male first
82 generation descendants of sire 3167). The survival data for each trial are shown in Table 1. In summary,
83 67.9% of the first generation offspring of 3167 and 51.1% of the second generation animals survived the
84 field challenge, compared to 8.7% of the unrelated cattle of the same breed across all field trials. Consistent
85 with the animals showing signs of infection and clinical symptoms (see methods for further details), body
86 temperatures typically peaked around day 15 following exposure (Fig 1). Comparing only animals that died
87 or survived without intervention, across the five field trials the offspring of sire 3167 were observed to be 3.3
88 times more likely to survive the exposure to *T. parva* than unrelated controls obtained from the same farm
89 (Mantel-Haenszel relative risk = 3.3, 95% confidence interval = 1.7, 6.44). We calculated the heritability (h^2)
90 of the tolerance phenotype among these animals by fitting survival status to sex and trial as fixed effects with
91 sire as a random effect. This model returned an estimated h^2 of 0.65 (s.e. = 0.57).

92 **Table 1. Summary of survival outcomes for control and pedigree animals over the course of five field**
93 **trials.**

Trial*	Controls				Sire 3167 offspring			
	Died	Euthanised	Treated	Survived	Died	Euthanised	Treated	Survived
2013	8	0	1	0	0	0	0	3
2014	9	4	0	1	3	0	3	4
2015	8	0	2	0	2	0	1	12
2017 [†]	2	1	3	1	4	0	3	17
2018 [†]	4	0	0	2	12	2	2	7
Total	31 (67.4%)	5 (10.9%)	6 (13%)	4 (8.7%)	21 (28%)	2 (2.7%)	9 (12%)	43 (57.3%)

94 * The first three field trials involved 1st generation offspring of sire 3167, whilst the field trials in 2017 and
95 2018 (indicated by a [†]) involved 2nd generation offspring.



96 **Fig 1. Heatmap of daily body temperature (°C) recordings throughout the field trials.** Animals 853,
97 919, 1148, 1456 and 1481 were all male progeny of sire 3167. Temperature observations commenced on day
98 2.

99 **Survival outcome is significantly associated with a region on**

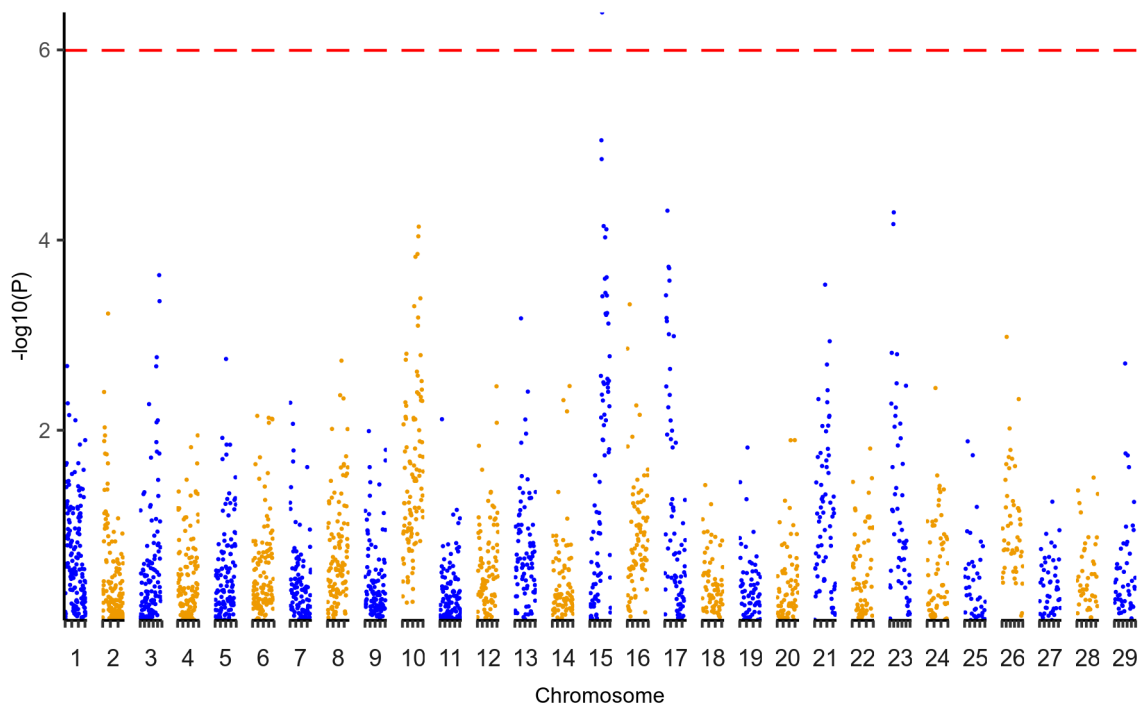
100 **chromosome 15**

101 We sought to identify loci underlying the heritable tolerance to *T. parva* within this pedigree. The founder of
102 the pedigree, sire 3167, was no longer available, and so his genotype probabilities (GP) were calculated from
103 the genotype frequencies of his offspring (see methods). Briefly, we generated whole-genome sequence
104 (WGS) data for 43 animals which included 28 1st generation animals, four animals subsequently identified as
105 likely 3rd degree relatives, and 11 unrelated animals. We genotyped a further 78 animals using the Illumina
106 BovineHD array, bringing the total number of animals to 121 comprising 28 1st generation, 47 2nd generation,
107 and 46 unrelated animals. After merging the datasets, filtering and correcting allele mismatches between the
108 WGS and BovineHD data, simulations were performed to calculate the GP of sire 3167 from the genotypes
109 of all 1st generation offspring. In total 465,938 SNPs were analysed and calculated to have a GP > 0.98, of
110 which 97% (n = 452168) had a GP > 0.9999, i.e. could be inferred with very high confidence. These GP
111 were used to impute genotypes for sire 3167, which were then merged with the genotype data of the pedigree
112 and unrelated animals and collectively phased while accounting for the known pedigree information.

113 The assumption in this study is that sire 3167 is carrying at least one genetic locus that confers tolerance to
114 *T. parva* infection. The pedigree could therefore inherit a tolerance haplotype from this founding bull, but we
115 did not want to exclude the possibility of it also being inherited down the maternal line. To do this, haplotype
116 analyses were conducted by first partitioning the phased genotype data into 1 Mb windows, for which the
117 Hamming distance of each animal's paternal and maternal haplotypes to each of those of sire 3167 was
118 calculated, resulting in four distance values per window for each animal. We fitted a regression model with
119 binomial survival outcome as a response to the four haplotype distances alongside sex, trial ID and sire to
120 account for these potential confounders. This allowed us to determine whether animals carrying particular
121 haplotypes that derived from, or that were highly similar to those of, sire 3167 were more likely to survive
122 exposure to *T. parva* infection.

123 We identified a genome-wide significant association ($p = 4.12 \times 10^{-7}$, adjusted for multiple testing via
124 permutations $p = 0.027$, see methods) on chromosome 15 (15:49-50 Mb; Fig 2), followed by two

125 neighbouring haplotypes (15:46-47 Mb unadjusted $p = 9.1 \times 10^{-6}$; 15:47-48 Mb unadjusted $p = 1.43 \times 10^{-5}$)
126 which although also nominally significant - were not significant genome-wide after correction (15:46-47 Mb
127 corrected $p = 0.23$; 15:47-48 Mb corrected $p = 0.32$). The paternally-derived 1 Mb haplotype windows of
128 surviving animals in this region (15:46-50 Mb) were more similar to both the A (median Hamming distance
129 $DA = 0.069 \pm 0.165$) and B ($DB = 0 \pm 0.160$) haplotypes of sire 3167 than those of the animals that
130 succumbed to infection ($DA = 0.254 \pm 0.250$; $DB = 0.278 \pm 0.258$).



131 **Fig 2. Regression analyses on haplotype distances.** Results of regression analyses of haplotypes versus
132 survival status. A single window crossed the corrected significance threshold determined from 1000
133 permutations, indicated by the dashed red line at $p < 0.05$.

134 **Characterisation of variants within the tolerance locus**

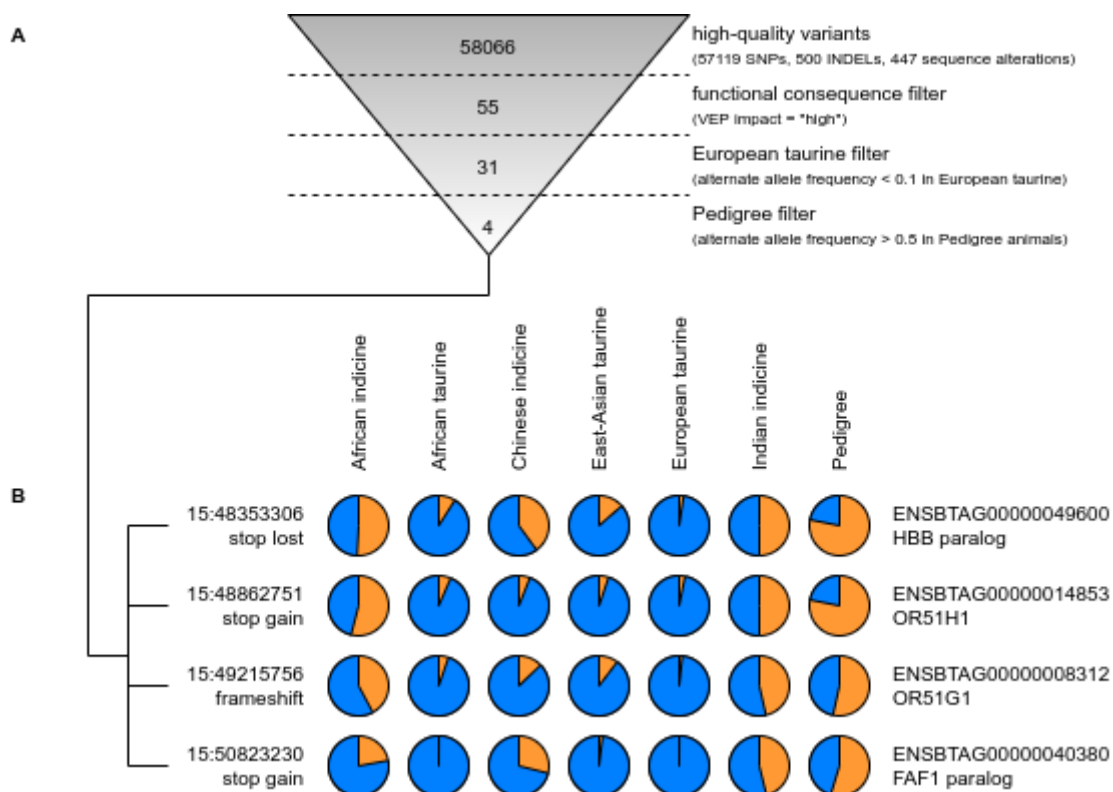
135 Having identified a genomic region significantly associated with survival outcome we next sought to identify
136 potential candidate functional variants within the locus for further investigation. To do this we characterised
137 both the impact of variants on coding regions as well as any potential link to the expression of nearby genes.
138 To define potential regulatory variants (eVariants) we sequenced mRNA extracted from white blood cells

139 collected from 29 animals (n = 23 pedigree, n = 6 unrelated) involved in the 2018 field trial at day 0 (i.e.
140 before their transport to Ol Pejeta Conservancy), day 7 and day 15. Within the target region, 720 variants
141 showed a nominally significant association between their genotype and the expression level of a nearby gene
142 on at least one of the timepoints (S1 Table), and a further 587 variants were tagged as potential response
143 eQTLs, where the association between genotype and gene expression differed between timepoints (S5
144 Table). However, none of these associations were significant after applying a false discovery rate correction
145 to account for multiple testing.

146 We next characterised the impact of the variants in this region on predicted coding regions. The allele
147 frequency and functional consequence of all SNPs spanning 1 Mb upstream and downstream of the identified
148 wider region (15:45-51 Mb) were characterised from the whole-genome sequence (WGS) data. After
149 filtering to retain high-quality variants, we identified 58066 variants and 235 genes in this region. These
150 included 57119 single nucleotide variants, 500 indels (an insertion or deletion, affecting two or more
151 nucleotides), and 447 sequence alterations (sequence ontology SO:0001059). A summary of all predicted
152 variant consequences is provided in the supporting information (S6 Table). From these, we selected 55
153 variants predicted to have a functional consequence with a high impact. As any variant conferring tolerance
154 to infection is unlikely to be present in non-native breeds, as evidenced by their extremely high mortality
155 when exposed to *T. parva*, we removed variants with an alternate allele frequency (aAF) > 0.1 in European
156 taurine breeds, leaving 31 variants. Similarly, we expected to observe the variant at a high frequency in the
157 1st generation offspring of sire 3167 that survived infection, and so removed variants with aAF < 0.5 in these
158 animals, resulting in 4 variants (Fig 3A): 1 frameshift variant, 2 stop gained and 1 start lost, each affecting a
159 different gene. Each of these variants had an alternate allele frequency < 0.04 in European taurine, < 0.091 in
160 African taurine breeds, but ranged from 0.22 to 0.54 in African and Asian indicine breeds, and from 0.53 to
161 0.78 in the pedigree of 3167 (Fig 3B).

162 Of the genes associated with these variants, two are olfactory receptors (*OR51HI* and *OR51GI*) and two are
163 novel genes - the first is a parologue of haemoglobin subunit beta (*HBB*) and the second a parologue of FAS-
164 associated factor 1 (*FAF1*). It should be noted we could not find any evidence of any of these genes being
165 expressed in white blood cell RNA-seq data, suggesting this is not their tissue of action. Olfactory receptors

166 (ORs) have been found to be involved in immune responses associated with the olfactory bulb, and there is
167 increasing evidence of OR expression in non-olfactory tissues, however there remains a significant gap in
168 our knowledge concerning the functional importance of ectopic ORs [12]. *HBB* is associated with
169 erythrocytes and variants in *HBB* have previously been linked to protection to human malaria, caused by
170 another pathogenic Apicomplexan protozoan, *Plasmodium falciparum*. However, as infection of
171 lymphocytes is responsible for the pathology of disease caused by *T. parva* and infected lymphocytes are
172 also the target of the protective acquired immune response, with infection of erythrocytes having little or no
173 role in either of these, the role of *HBB* tolerance to *T. parva* infection is not immediately obvious. In contrast,
174 *FAS* is a member of the TNF-receptor superfamily involved in apoptosis, and *T. parva*-infected cells have
175 previously been shown to be resistant to *FAS*-induced cell death [13]. Thus, we focused on further examining
176 the association of the variant in the *FAF1* paralog with tolerance to *T. parva* infection.



177 **Fig 3. Prioritisation of variants.** (A) Successive filters were applied to the high-quality variants in the
178 region identified as significantly associated with tolerance to *T. parva* infection (15:45-51 Mb). This reduced

179 the number of variants from 93960 to four predicted to have a high functional consequence, a low alternate
180 allele frequency (aAF < 0.1) in European taurine animals, and a high alternative allele frequency in Pedigree
181 animals (aAF > 0.5). (B) The allele frequencies (reference allele in blue, alternative allele in orange) of these
182 four variants were subsequently calculated in different populations, indicating the alternative allele is
183 potentially of an indicine origin.

184 **Genotyping of the *FAF1* paralog confirms a significant association
185 with survival outcome**

186 The *FAF1* paralog shares 96.75% identity with 68.77% of *FAF1*'s nucleotide sequence. The stop gain variant
187 (15:50823230 on ARS-UCD1.2) in the *FAF1* paralog (referred to here as *FAF1B*) converts an arginine codon
188 (cga) to a stop codon (tga) which would result in a truncated protein. Within *FAF1* itself there is no variant
189 recorded in dbSNP at the homologous base position (3:95786449) to the *FAF1B* variant (15:50823230). The
190 *FAF1B* variant is not present on the BovineHD array used to genotype the majority of the animals. To
191 establish if there is a significant association between genotype and survival outcome across the wider set of
192 animals, we designed primers to amplify and sequence this variant in 57 trial animals that were not
193 previously whole-genome sequenced, bringing our genotype data for *FAF1B* to 100 animals. These animals
194 include 77 pedigree (43 survived, 34 succumbed to infection) and 23 unrelated individuals (4 survived, 19
195 succumbed to infection). In all, 88% of the animals homozygous for the variant allele (T/T) survived the
196 field challenge (7 out of 8, the final animal having been treated rather than having died from the infection),
197 compared to 62% (36 out of 58) of heterozygotes (C/T) and only 12% (4 out of 34) of those homozygous for
198 the reference allele (C/C; Table 2). Analysis by logistic regression of survival status versus genotype at this
199 variant was significant across all animals (likelihood ratio test $p = 2.48 \times 10^{-4}$), within unrelated animals
200 (likelihood ratio test $p = 5.38 \times 10^{-4}$), and within the pedigree (likelihood ratio test $p = 6.34 \times 10^{-4}$), when
201 controlling for sex, trial, sire (where pedigree animals involved), including 3rd degree relatives in the
202 pedigree, and classifying animals that received treatment or were euthanised as having died.

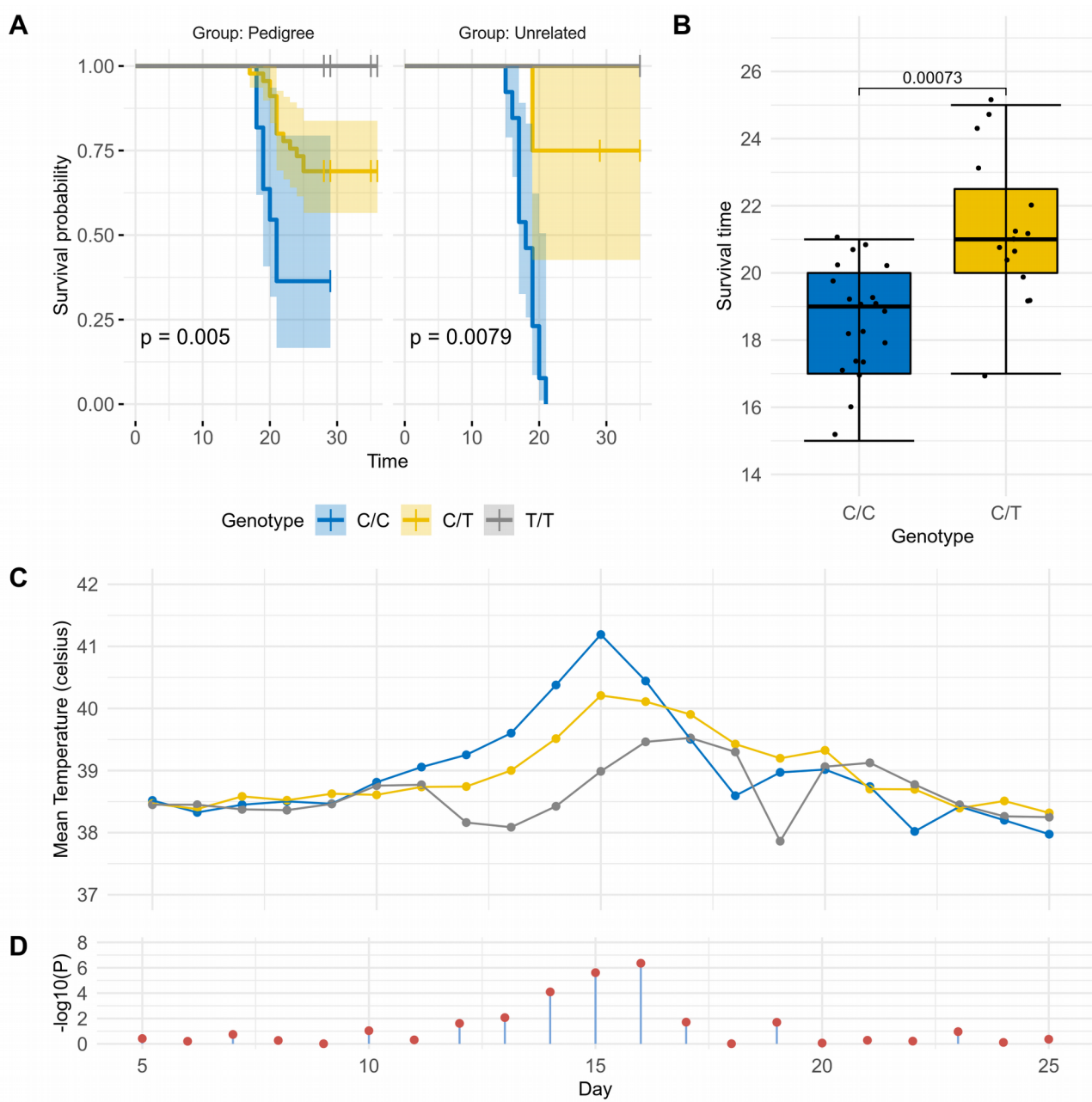
203 Considering explicitly the unrelated and pedigree (1st and 2nd generation) animals that survived or succumbed
204 to infection, a comparison of survival curves fitting survival time versus genotype at the *FAF1B* variant while

205 accounting for degree of relatedness returns a significant association (log-rank $p = 4.13 \times 10^{-13}$; Fig 4A).
206 Further to its association with survival, among these animals that succumbed to the disease, those
207 heterozygous at the variant succumbed significantly (Mann-Whitney U test $p = 7.3 \times 10^{-04}$) later on average
208 than homozygous reference animals (mean of 21.27 ± 2.25 days versus 18.55 ± 1.7 days; Fig 4B). An
209 animal's genotype at this variant was also observed to be associated with their temperature over the course of
210 the infection (Fig 4C), with T/T animals generally showing a lower increase in temperature, and in particular
211 at days 15 and 16 (ANOVA F test P of 2.44×10^{-06} and 4.43×10^{-07} respectively when accounting for
212 relatedness, sex and trial. Fig 4D).

213 **Table 2. The genotype counts of the *FAF1B* variant.**

Genotype	Status	Unrelated	3 rd degree*	2 nd gen.	1 st gen.	Total
C/C	Succumbed	13	2	7	0	22 (64.7%)
C/C	Euthanised	2	0	1	0	3 (8.8%)
C/C	Treated	3	0	2	0	5 (14.7%)
C/C	Survived	0	0	4	0	4 (11.8%)
C/T	Succumbed	1	0	9	5	15 (25.9%)
C/T	Euthanised	0	0	1	0	1 (1.7%)
C/T	Treated	0	0	3	3	6 (10.3%)
C/T	Survived	3	2	16	15	36 (62.1%)
T/T	Succumbed	0	0	0	0	0 (0%)
T/T	Euthanised	0	0	0	0	0 (0%)
T/T	Treated	0	0	0	1	1 (12.5%)
T/T	Survived	1	0	2	4	7 (87.5%)

214 * Upon genotyping, four controls were determined to in fact likely be 3rd degree relatives of sire 3167, these
215 are separated out in the above table. Note there were no homozygote C/C first generation animals as sire
216 3167 was T/T at this variant.



217 **Fig 4. Survival analyses for the *FAF1B* variant in pedigree (1st and 2nd generation) and unrelated**
 218 **animals.** (A) Analysis of survival curves in animals that succumbed or survived *T. parva* infection reveals
 219 significant associations between survival probability and genotype. Log-rank p values are reported.
 220 Comparing survival curves when fitting survival time against genotype whilst accounting for relatedness
 221 (unrelated, 1st generation, 2nd generation) returns log-rank $p = 4.13 \times 10^{-13}$. (B) Comparison of survival time
 222 versus genotype for animals that succumbed to infection. The mean survival time for C/C animals was 18.55

223 ± 1.7 days, while mean survival time for C/T animals was 21.27 ± 2.25 days. A Mann-Whitney U test p value
224 is reported. (C) Mean temperature versus field trial day for all animals regardless of survival outcome and
225 relatedness, grouped by genotype. Temperature peaked at day 15 in C/C and C/T animals, and at day 16 in T/
226 T animals. (D) Fitting T allele count against temperature whilst accounting for relatedness, sex and trial,
227 returns significant associations from days 13 to 16 (ANOVA F-test $p < 0.01$) .

228 To determine how much variance in heritability is explained by the *FAF1B* SNP we ran linear mixed effect
229 models using residual maximum likelihood to estimate parameters. Having calculated the heritability (h^2)
230 based on phenotypic data alone as 0.65 (s.e. = 0.57) as stated above, we subsequently accounted for genetic
231 effects by fitting the genotype at the *FAF1B* SNP as a fixed effect. This model returned a significant additive
232 SNP effect of $\alpha = 0.43 \pm 0.083$ for a single copy of allele T. This is highly significant assuming an additive
233 model $t = 5.2$ (Student's left-tailed t-distribution $p = 2.51 \times 10^{-6}$), with no evidence for a dominant effect
234 ($\text{dom} = 0.12 \pm 0.09$) $t = 1.25$ (Student's left-tailed t-distribution $p = 0.18$).

235 ***FAF1B* genotype-associated tolerance replicated in independent 236 population**

237 We next investigated any evidence for replication of this association in the independent Infectious Disease of
238 East African Livestock (IDEAL) cohort. The IDEAL study was conducted in a *T. parva*-endemic area in
239 western Kenya in 2007 in a smallholder system free of buffalo, and involved the intensive monitoring of 548
240 East African Shorthorn Zebu (EASZ) calves for the first year of life. The study generated data on the
241 frequency and clinical signs of infections and their impact on health and growth [14], with 32 calves
242 determined, by clinical signs and post mortem observations, to have died of ECF. There were a number of
243 important differences between this study and the field trials reported above. The animals in the IDEAL study
244 were spread across farms and different environmental exposures and, unlike the Boran breed, EASZ are
245 believed to exhibit generally elevated tolerance to ECF - supported by the IDEAL project reporting a 6%
246 mortality due to *T. parva* infection despite 76% of animals becoming infected in their first year of life [15].
247 Furthermore, transmission of *T. parva* in the IDEAL study will have been via tick transmission from cattle to

248 cattle, rather than transmission to cattle from ticks that had previously fed on buffalo as in the field trials. We
249 genotyped 130 EASZ at the *FAF1B* SNP using the same primers as for the Boran. This included the 32
250 calves that died of ECF, and 98 randomly selected survivors from the IDEAL study. Consistent with the field
251 trial results suggesting the T allele is associated with tolerance, no homozygote T/T animals in the study
252 succumbed to ECF (Table 3). Logistic regression of survival status versus genotype while accounting for the
253 animal's sex and the latitude, longitude, and elevation of the sampling location was significant in this cohort
254 of 130 animals (likelihood ratio test $p = 0.029$) with the same direction of effect as in the 3167 pedigree.

255 **Table 3. IDEAL cohort genotypes.**

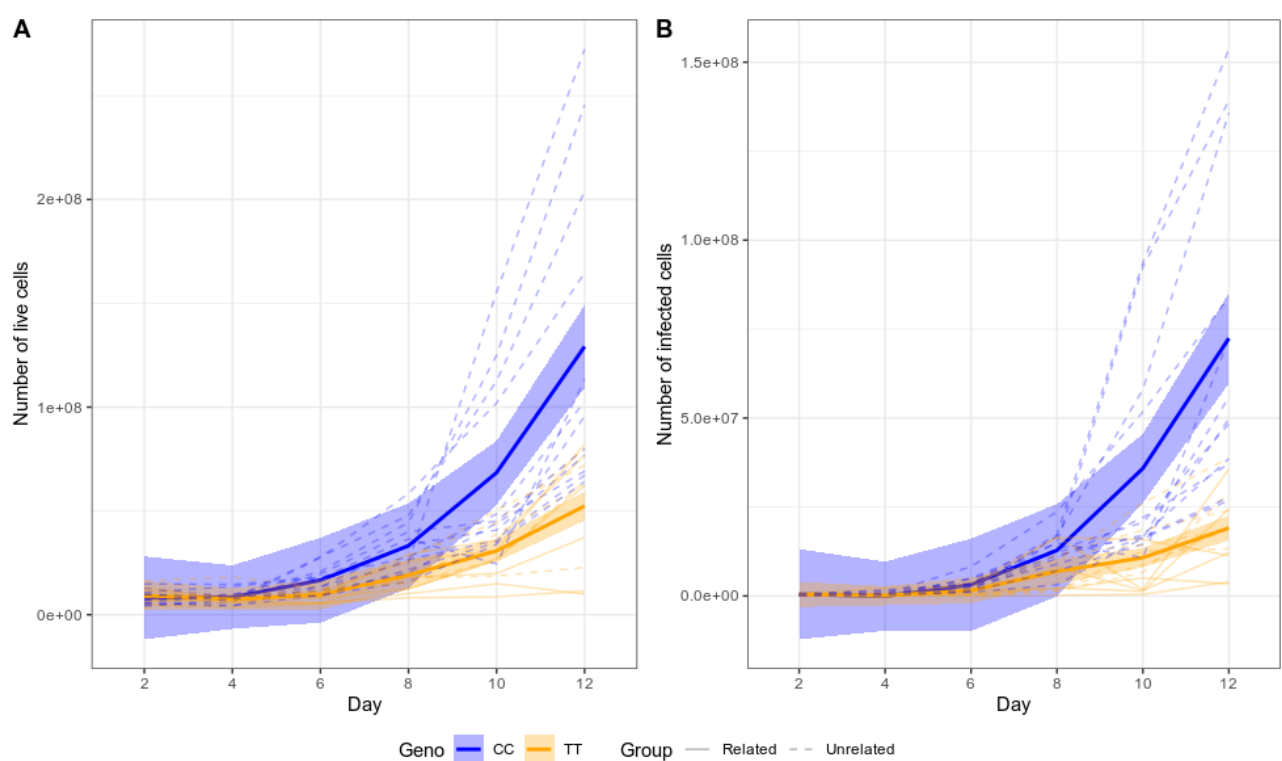
Genotype	Succumbed to ECF (n = 32)	Survived [†]	
		Episode (n = 31)	No-episode (n = 67)
C/C	16 (50%)	21 (68%)	30 (45%)
C/T	16 (50%)	8 (26%)	27 (40%)
T/T	0 (0%)	2 (6.5%)	10 (14.9%)

256 [†] Randomly selected animals that survived are further categorised according to whether or not they presented
257 any evidence of a clinical episode associated with ECF, which include: pyrexia, and hypertrophic parotid and
258 prescapular lymph nodes.

259 ***FAF1B* genotype is associated with live cell count and *ex vivo* infection
260 level**

261 The *in vitro* expansion of *T. parva*-infected cells obtained from cattle surviving infection is lower than the
262 expansion of cells in cattle succumbing infection [16]. We therefore sought to determine if there is also a
263 difference in the *in vitro* expansion of *T. parva*-infected cells based on the *FAF1B* genotype of the animals.
264 Peripheral blood mononuclear cells (PBMCs) were cultured and infected by incubation with salivary glands

265 dissected from *R. appendiculatus* fed on animals infected with *T. parva*. The level of infection in ticks was
266 estimated by counting the number of infected acini in a sample of dissected salivary glands, and the
267 sporozoite suspension adjusted to a concentration equivalent to 2000 infected acini per ml [see 17]. Equal
268 volumes of sporozoites and cells (2×10^7 PBMCs) were cultured from 12 cattle unrelated to 3167 carrying
269 the C/C genotype at the *FAF1B* SNP, and 12 cattle carrying the T/T genotype, which comprised of six
270 animals from the tolerant pedigree and a further six unrelated animals for comparison. Counting of cells
271 stained with trypan blue every 2 days over a period of 12 days revealed a significant association between live
272 cell count and genotype when fitting day as an interaction term and accounting for relatedness (see methods,
273 F-test $p = 1.42 \times 10^{-7}$; Fig 5A). To determine if there was a difference in infectivity associated with the
274 *FAF1B* SNP, cells were stained with a fluorophore directed at the polymorphic immunodominant molecule
275 (PIM) expressed on the *T. parva* schizont's surface. As with the live cell count, a significant association
276 between the proportion of infected (PIM+) cells and genotype was observed when fitting day as an
277 interaction term and accounting for relatedness (F-test $p = 7.56 \times 10^{-9}$; Fig 5B).



278 **Fig 5. Cell expansion and infectivity levels in cultured cells infected with *T. parva*.** (A) Animals
279 possessing a C/C genotype at the *FAF1B* SNP exhibit higher live counts throughout the course of infection
280 compared to T/T animals. The association between live cell count and genotype when fitting day as an
281 interaction term and accounting for relatedness is significant (F-test $p = 1.42 \times 10^{-07}$). (B) In addition,
282 animals possessing a C/C genotype exhibit a higher proportion of infected (PIM+) live cells, which is also
283 significant (F-test $p = 7.56 \times 10^{-09}$). Thin dashed lines indicated unrelated animals, solid, thin lines indicate
284 animals from the ECF-tolerant pedigree. The blue and orange ribbons and thick blue and orange lines
285 indicate the 95% confidence interval around the mean for C/C and T/T genotypes, respectively.

286 Consequently, these data suggest the association of the *FAF1B* locus with survival in the 3167 and IDEAL
287 cohorts may also be reflected in different capacities of *T. parva*-infected cells to establish and expand *in*
288 *vitro*.

289 **Discussion**

290 The progeny of sire 3167 demonstrate a clear, heritable tolerance to buffalo-derived *T. parva* infection, which
291 haplotype-based analyses reveal to be significantly associated with an extended 6 Mb genomic region on
292 chromosome 15. Notably, this same region was one of a small number showing evidence of between-breed
293 selective sweeps in both cattle and water buffalo in a recent study [18], and both species are susceptible to a
294 closely related *Theileria* species, *T. annulata*. This, along with the elevated non-reference allele frequency
295 among indicine cattle breeds at variants in this region, raises the possibility that the tolerance phenotype first
296 arose as a response to *T. annulata*, which is transmitted by a different tick and is present in a region
297 extending from north Africa and southern Europe into the Middle East and Asia. This was then introduced
298 into Africa in one of the waves of introduction of *Bos indicus* breeds. Within this genomic region we
299 identified a putative stop-gained polymorphism within a parologue of the *FAF1* gene, *FAF1B*, of which the
300 genotype is significantly associated with survival outcome. As *FAS*-induced apoptosis has previously been
301 shown to be targeted by the parasite to facilitate the transformation of T cells [13], this gene is a plausible
302 candidate for a central role in mediating tolerance. We also find the *FAF1B* SNP to be associated with cell
303 expansion and infection levels *in vitro*. A key hallmark of *T. parva* infection is it leads to the uncontrolled

304 proliferation of T-cells and, although further work is required, these *in vitro* findings potentially support the
305 idea that the tolerance phenotype is linked to better management of the uncontrolled proliferation of infected
306 cells.

307 It should be noted we could find no evidence that *FAF1B* is expressed in white blood cells (WBCs) before or
308 after infection, though its action could be in other tissues. Although we found little evidence for any eQTLs
309 in this region potentially driving the phenotype, this analysis had limitations in that the sample size was
310 small, blood is potentially confounded by cell-type composition differences, and, although a reasonable
311 candidate, blood may not be the tissue of action. Consequently, further work is required to elucidate any
312 causal relationship between this *FAF1* parologue and the enhanced tolerance to *T. parva* linked to this locus.
313 Irrespective of whether it is driving tolerance though, we have demonstrated the putative stop gained variant
314 in this gene is strongly linked to the tolerance phenotype and importantly provides a potential effective
315 genetic marker for breeding for tolerance. Notably, of the combined total of 20 animals that were
316 homozygous for the alternate allele at this locus across the Boran pedigree, controls and EASZ, none
317 succumbed to *T. parva* infection (though one was treated). This is in contrast to the 53% of animals which
318 were homozygote for the reference allele (n = 44) that succumbed (n=83). Although a number of these
319 animals were related, the lack of deaths among homozygote carriers adds support to the promise of potential
320 breeding for tolerance using this allele. It is also worth noting that of the four identified 3rd degree relatives,
321 only the two that possessed a T allele survived infection. Furthermore, those heterozygote carriers that
322 succumbed to the disease were observed to survive several days longer on average than animals carrying no
323 copies of the variant, and to display some evidence of potentially showing fewer clinical episodes in the
324 IDEAL cohort. *T. parva* can be transmitted via ticks that have previously fed on either infected cattle or
325 infected African buffalo. The challenge in the field trials was buffalo-derived, as cattle had been absent from
326 the trial site prior to the introduction of the trial animals. In contrast the challenge in the IDEAL study was
327 cattle-derived. Consequently, the evidence points towards this locus being potentially protective against
328 disease caused by both forms of the parasite.

329 We have therefore validated a genetic marker which is significantly associated with survival outcome. This
330 marker can consequently be applied to support selective breeding programmes with a view to improving the

331 tolerance of cattle populations, in order to reduce the substantial impact of *T. parva* on sub-Saharan African
332 countries. Confirmation of the functional variant in this region will facilitate the application of modern gene
333 editing technologies to formally demonstrate the functional role of the variant and ultimately to rapidly
334 increase its frequency in imported, productive cattle throughout Africa.

335 **Methods**

336 The study protocols were approved by ILRI's Institutional Animal Care and Use Committee (References
337 2013-03, 2014-32, 2015-29, 2017-02, 2018-10).

338 **Field trials**

339 Field trials involved transporting animals from the Kapiti Research Station in Machakos county, a region
340 largely free of ECF, to the Ol Pejeta Conservancy (Kenya) in a region endemic for *T. parva*. The study site
341 where animals remained for up to 35 days was free of other cattle but populated by African buffalo [11]. The
342 2013, 2014 and 2015 field trials involved 1st generation progeny of sire 3167 while the 2017 and 2018 field
343 trials involved progeny of males sired by 3167; in all trials unrelated animals were also included, and
344 researchers conducting the phenotyping were unaware as to which animals were pedigree or unrelated.
345 Although pedigree records were maintained throughout, for the 2017 and 2018 field trials animals were
346 genotyped in advance to verify their relatedness. Genetic analyses (described below) identified 21
347 individuals that were incorrectly documented as belonging to the pedigree of sire 3167; eight pedigree
348 individuals whose sire was incorrectly recorded, but which remained within the pedigree; and seven
349 individuals thought to be unrelated but which were found to be 3rd degree relatives from four sibships.
350 Animals in all field trials were screened in advance to ensure they tested negative by ELISA [19] for
351 antibodies against *T. parva* and, for the last four trials, *T. mutans*, and in addition in the 2013 [11], 2017 and
352 2018 field trials by p104 PCR [20] to test for active *T. parva* infection. During the field trials body
353 temperature recordings were taken on a daily basis. On a small number of occasions a recording could not be
354 taken due to the temperament of the animal. The first four days of temperature recordings were excluded
355 from downstream analyses as these typically exhibited unusual deviations due to the stress of transport. A

356 summary of phenotypic data for field trial animals analysed in this study is provided in S1 Table 1, along
357 with temperature observations in S2 Table.

358 The most likely cause of death for the first study was reported to be buffalo-derived *T. parva* infection, based
359 on clinical signs and post mortem observations [11]. Similar observations were made in the subsequent
360 studies. All animals exhibited pyrexia except one (4150; Fig. 1), and swollen parotid and prescapular lymph
361 nodes, whilst laboured breathing, nasal discharge and corneal opacity were commonly observed.
362 Microscopic examination of aspirates from the parotid or prescapular lymph nodes revealed *T. parva*
363 macroschizonts in at least one lymph node of every animal. Routine post mortem observations included
364 frothy exudate in the trachea and pulmonary oedema. Seroconversion to anti-*T. parva* antibodies was
365 detected in 46 of the 47 surviving animals and in 42 of the 74 animals that succumbed.

366 Survival risk ratios were calculated from a fixed-effects (Mantel-Haenszel) meta analysis of animals that
367 survived or died, without intervention, using the meta.MH function of the rmeta package for R. To address
368 zero values for unrelated survivors in field trials 2013 and 2015, a zero-cell correction was applied by adding
369 0.5 to all values [21].

370 **Sampling**

371 Blood was collected from the animals in EDTA tubes and extracted using DNEasy® Blood and Tissue Kits
372 (Qiagen) according to manufacturer's instructions. For genotyping on the Illumina BovineHD BeadChip,
373 DNA integrity was first assessed by electrophoresis on a 1.5% agarose gel, and quantitated by NanoDropTM
374 spectrophotometer for dilution to a concentration of 50 ng/µl in 40µl of elution buffer. DNA samples were
375 shipped to Edinburgh Genomics where quality was assessed by PicoGreenTM assay prior to genotyping. For
376 whole-genome sequencing DNA was extracted using the MagNA Pure LC Total Nucleic Acid Isolation Kit
377 (Roche Diagnostics GmbH).

378 **Survival analysis**

379 Survival analyses were performed and plotted in R [22] (v3.4.4) using the survminer (v0.4.6) package.
380 Briefly, a survival object was constructed excluding animals that were treated or euthanised fitting survival

381 time, defined in days as either the end of the field trial or the day on which the animal died, against genotype
382 whilst accounting for degree of relatedness (unrelated, 1st or 2nd generation). P values were calculated from
383 the fitted survival curves using the log-rank method.

384 **Processing of whole-genome sequence data**

385 Sequencing was performed on the Illumina HiSeq X platform using 150bp pair end reads with 550bp insert,
386 TruSeq PCR free libraries, to a target depth of 30X. Sequence reads were aligned to the ARS-UCD1.2
387 assembly using BWA-MEM [23] (v0.7.17), and processed using GATK [24,25] (v4.0.8.0) applying
388 MappingQualityNotZeroReadFilter, MarkDuplicates, and base quality score recalibration (BQSR) using
389 known sites from the 1000bulls genome project (<http://www.1000bulldgenomes.com/>). Variants were called
390 using HaplotypeCaller [26,27] to generate gVCF files, from which joint variant calling was performed across
391 samples, followed by variant quality score recalibration (VQSR).

392 **Processing of BovineHD genotyping data**

393 Genomic coordinates for the Illumina BovineHD Genotyping BeadChip were updated from the UDM3.1
394 reference assembly to the newer ARS-UCD1.2 assembly using data provided by Robert Schnabel from the
395 University of Missouri (UMC_marker_names_180910.zip, available at
396 https://www.animalgenome.org/repository/cattle/UMC_bovine_coordinates/). The array data was converted
397 from PED to VCF format using Plink [28] (v1.90blg). A Python script was written to cross-reference the
398 alleles for SNPs from the genotype data against those from the sequence data, to correct for discrepancies in
399 reference allele and/or strand between the different datasets. SNPs with alleles whose concordance could not
400 be validated (A/T, T/A, C/G, G/C) were discarded. The VCFs from genotyping and sequencing were
401 subsequently merged using bcftools [29] (v1.2), and filtered to remove SNPs with a minor allele frequency
402 (MAF) < 0.05 and call rate < 0.95.

403 **Analysis of relatedness**

404 To cross-validate the written breeding records and ensure that individuals were not assigned to the pedigree
405 of sire 3167, incorrectly, the genotype data were analysed using VCFtools [30] (v0.1.13) to calculate
406 relatedness as per Manichaikul et al. [31]. Relatedness values range from $\Phi < 0.0442$ for unrelated
407 individuals, $0.0442 < \Phi < 0.0884$ for 3rd degree relatives, $0.0884 < \Phi < 0.177$ for 2nd degree relatives, and Φ
408 > 0.1777 for 1st degree relatives.

409 **Imputation of founding sire 3167**

410 Genotypes from the 1st generation offspring were phased with SHAPEIT2 [32] (v2r837) using a genetic map
411 estimated from physical SNP positions assuming 1 cM/Mb, employing a window size (-W) of 5 Mb, and the
412 duoHMM [33] (v0.1.7) algorithm to take into account the available pedigree information. A Python script
413 was written to estimate sire 3167's genotype probabilities from the 1st generation genotypes. For each SNP, 1
414 million simulations were performed to generate genotypes for 34 individuals (the number of 1st generation
415 offspring genotyped). During each iteration, for each individual a 'paternal' allele was randomly chosen from
416 each of sire 3167's possible genotypes {0/0, 0/1, 1/1}, and combined with a random 'maternal' allele {0, 1}.
417 Thus, for each iteration we recorded the counts of offspring for each combination of alleles {0/0, 0/1, 1/1}
418 for each of sire 3167's possible genotypes. The simulations incorporated a 5% error rate which would cause
419 the paternal allele to be switched. From these simulations, the offspring genotype counts that matched those
420 of the 1st generation data were retrieved for each of sire 3167's possible genotypes, and the frequency of each
421 recorded as sire 3167's genotype probabilities. Sire 3167's genotypes were then imputed from these
422 probabilities and the 1st generation phased genotype data in 5 Mb windows using IMPUTE2 [34] (v2.3.2).
423 The imputed genotypes for sire 3167 and the 1st generation genotype data were then combined with the 2nd
424 generation genotype data, and collectively phased using SHAPEIT2 and duoHMM.

425 **Haplotype association analyses**

426 Assuming sire 3167 carries one or more haplotypes associated with tolerance to *T. parva*, we partitioned the
427 genotype data into 1 Mb 'haplotype blocks' and calculated the Hamming [35] distance for each progeny's

428 paternal (A) and maternal (B) haplotypes (h) to those imputed for sire 3167 (r). This resulted in four
429 haplotype distance metrics per individual { A_h, A_r ; A_h, B_r ; B_h, A_r ; B_h, B_r } which were divided by the number of
430 SNPs in the haplotype to correct for the varying SNP density of haplotypes. The analysis was performed in R
431 using the proxy (v0.4-22) package. Multiple regression was performed in R to test binomial survival status
432 against the four haplotype distances with sex, field trial and sire fitted as covariates. This model was then
433 compared to a reduced model without the four haplotype distances included using ANOVA. Individuals that
434 received veterinary intervention due to their severe symptoms, or were euthanised, were treated as non-
435 survivors for the purpose of this binary phenotype. To determine significance thresholds that account for
436 multiple testing 1000 permutations were performed where the set of four distances were permuted between
437 individuals. For all blocks on the same chromosome the distances were swapped between the same sets of
438 animals to maintain their relationship across regions. Thus, the phenotypic metadata remained associated
439 with the correct ID and any linkage between haplotypes along a chromosome remained intact. The minimum
440 p value observed across all blocks in the genome for each permutation was recorded, from which a 0.05
441 significant threshold was determined as the value where just 5% of these values were smaller (S3 Table).

442 Expression quantitative trait loci (eQTL) analyses

443 RNA was extracted from white blood cells of animals sampled during the 2018 trial prior to being
444 transported to the field site (day 0) and on days 7 and 15 of the field trial. These animals included 15 that
445 succumbed to infection, 9 that survived, 2 that were euthanised and 2 that were treated. Following phenol
446 chloroform extraction, mRNA was sequenced on the Illumina HiSeq platform to generate ~70M x 50 bp
447 reads per sample. RNA sequencing reads were aligned to ARS-UCD1.2 using STAR [36] (v2.7.1a;).
448 Stranded fragments per kilobase of exon model per million reads mapped (FPKM) values were calculated for
449 exon features from the alignments using Htseq-count [37] (v0.11.2;). FPKM values were tabulated and
450 filtered in R for each sampling day to retain only genes where at least 50% of samples had FPKM \geq 3.
451 Response expression quantitative trait loci (reQTL) analyses were performed in R as follows. Genes within
452 the region 15:44-52 Mb were identified, and for each day the FPKM of each gene for each individual was
453 retained, along with the allele dosages for *cis* variants - these included any bi-allelic SNP with MAF > 0.1
454 within 1 Mb upstream of the gene's start position to 1 Mb downstream of its end position. SNP allele

455 dosages were derived from the genotype data generated using the BovineHD array described above. Animals
456 were assigned a group value of ‘pedigree’ or ‘control’, and for each day we regressed a gene’s FPKM values
457 against the allele dosages of each of its *cis* variants independently, while accounting for an individual’s sex
458 and group assignment. To identify reQTL we used a beta-comparison approach. Here we performed pairwise
459 comparisons of regression slopes for an eQTL at the different time points in a z-test:

$$Z = \frac{\beta_x - \beta_y}{\sqrt{\delta_x^2 + \delta_y^2}}$$

460 To test which genes exhibited significantly different expression between survivors and those that succumbed
461 to infection by *T. parva*, for each gene within the region we ran logistic regression fitting binomial survival
462 status against FPKM adding sex and group as covariates. This was compared to a reduced model without
463 FPKM, by ANOVA and the likelihood ratio test.

464 **Prioritisation of candidate variants**

465 Publicly available WGS data for 421 cattle [18] were processed as described above, combined with the WGS
466 data for 43 cattle generated for this study, and variants jointly called. Additional filtering beyond that
467 described above included extracting the target interval 15:45095457-51095457, the removal of singletons
468 and of variants with a genotype quality (GQ) < 30, a minor allele frequency (MAF) < 0.01 or missingness ≥
469 0.05. This resulted in the removal of 11 cattle and 1 variant due to missingness, and 277 variants due to low
470 MAF. After filtering, stratified allele frequencies were calculated using Plink for the remaining 93682
471 variants across 453 cattle that represented different backgrounds (Boran pedigree, African taurine, African
472 indicine, Chinese indicine, East-Asian indicine, European taurine, Indian indicine, and cattle from the
473 Middle East). The functional consequence of variants was determined using Ensembl’s Variant Effect
474 Predictor [38] (VEP).

475 **Primer design and PCR amplification**

476 Primers to genotype the candidate variant were designed using Primer3Plus [39]
477 (<https://primer3plus.com/cgi-bin/dev/primer3plus.cgi>) and checked for specificity by a BLAT search against

478 the reference genome (ARS-UCD1.2). The primers Pair1_L (5'GCTTGGGATCTGACAAAGGA3') and
479 Pair1_R(5'TGGCCTCACGTTCTTCTT3'), synthesized at Macrogen Europe, amplified a 382bp
480 fragment. Genomic DNA was extracted from blood samples using DNeasy Blood & Tissue Kit (Qiagen,
481 Germany) according to the manufacturer's instructions. A 25 μ l PCR mix was prepared using 12.5 μ l
482 OneTaq® Quick-Load® 2X Master Mix (New England Biolabs) with Standard Buffer, 9.5 μ l of nuclease-free
483 water, 0.5 μ l of each 10 μ M primer (Pair1_L and Pair1_R) and 2 μ l of genomic DNA extract. The PCR was
484 performed using an AllInOneCycler™ (Bioneer) with the following conditions: initial denaturation at 94°C
485 for 30 seconds; 30 cycles of denaturation at 94°C, annealing at 58°C and extension at 68°C for 30 seconds at
486 each step; the final extension at 68°C for 5minutes. PCR products were sent to Macrogen Europe
487 (Amsterdam, Netherlands) for sequencing.

488 **Heritability analyses**

489 The heritability analysis was performed using ASReml (v4.2; <https://asreml.kb.vsni.co.uk/>) by fitting the
490 fixed effects of sex and field trial year, with sire as a random effect. Genotype was included as a fixed effect
491 when accounting for genetic effects. We also estimated the additive and dominance effects of each SNP.
492 Defining AA, BB and AB to be the predicted trait values for each genotype class, p and q to be the SNP
493 allele frequencies, the genetic effects were then calculated as follows: additive effect, $a = (AA - BB)/2$ and
494 dominance effect, $d = AB - [(AA + BB)/2]$.

495 **Cell *in vitro* expansion and infection**

496 Peripheral blood mononuclear cells (PBMC) were isolated from venous blood and cryopreserved in liquid
497 nitrogen. Detailed methods on the *in vitro* experiments are described in Latre de Late *et al.* [16]. Briefly, cells
498 were suspended in complete RPMI culture medium and infected with *T. parva* by incubation with freshly
499 dissected salivary glands from *R. appendiculatus* fed on animals infected with *T. parva* Muguga, stabilate
500 3087, as previously described [40]. Tick infection levels were estimated by counting the number of infected
501 acini in a sample of dissected salivary glands, and the sporozoite suspension adjusted to a concentration
502 equivalent to 2000 infected acini per ml [17]. During each experiment, cells from C/C and T/T animals were

503 infected with the same batch of sporozoites. Equal volumes of sporozoites and cells (2×10^7 PBMCs) were
504 mixed and incubated at 37°C for 90 min with periodic mixing. Cells were centrifuged, washed, and
505 resuspended in culture medium as described. Cells were maintained in T25 flasks with fresh culture medium
506 added every 2 to 3 days. Live cells in cultures were quantified by trypan blue staining every two days for 12
507 days. To quantify live, infected cells in culture, the infrared dye LIVE/DEAD™ Fixable Near-IR Dead Cell
508 Stain (ThermoFisher Scientific) was first used to identify dead cells for removal, and the remaining live cells
509 were stained with monoclonal antibody IL-S40.2, which recognises the polymorphic immunodominant
510 molecule (PIM) expressed on the schizont surface. Fluorescence data were acquired for 105 cells per sample
511 using a BD FACSCanto II flow cytometer (Becton Dickinson, Belgium) ,and analysed using Flow Jo
512 software (FlowJo, LLC, Oregon, USA).

513 **Acknowledgements**

514 This research was conducted as part of the CGIAR Research Program on Livestock. ILRI is supported by
515 contributors to the CGIAR Trust Fund. CGIAR is a global research partnership for a food-secure future. Its
516 science is carried out by 15 Research Centers in close collaboration with hundreds of partners across the
517 globe (www.cgiar.org). Some of the work described in this paper was supported by grant BB/H009515/1
518 awarded jointly by the then UK Department for International Development and the UK Biotechnology and
519 Biological Sciences Research Council (BBSRC) under the Combating Infectious Diseases of Livestock for
520 International Development (CIDLID) program. This research was funded in part by the Bill & Melinda
521 Gates Foundation and with UK aid from the UK Foreign, Commonwealth and Development Office (Grant
522 Agreement OPP1127286) under the auspices of the Centre for Tropical Livestock Genetics and Health
523 (CTLGH), established jointly by the University of Edinburgh, SRUC (Scotland's Rural College), and the
524 International Livestock Research Institute (ILRI). The findings and conclusions contained within are those of
525 the authors and do not necessarily reflect positions or policies of the Bill & Melinda Gates Foundation nor
526 the UK Government. This work was also supported by funding from the BBSRC (BBS/E/D/30002275). The
527 authors are very grateful to the management of the Ol Pejeta Conservancy, Private Bag, Nanyuki 10400,
528 Kenya for allowing us to perform the field studies. The authors would also like to thank Mingyan Yu and
529 Cynthia Onzere of ILRI, for preparing the DNA samples for the genomic analyses.

530 References

1. Gachohi J, Skilton R, Hansen F, Ngumi P, Kitala P. Epidemiology of East Coast fever (Theileria parva infection) in Kenya: past, present and the future. *Parasit Vectors*. 2012;5: 194. doi:10.1186/1756-3305-5-194
2. McLeod R, Kristjanson P. Economic Impact of Ticks and Tick-Borne Diseases to Livestock in Africa, Asia and Australia. In: ACIAR - Australian Centre for International Agricultural Research [Internet]. 14 Feb 2017 [cited 1 Feb 2019]. Available: <https://www.aciar.gov.au/node/13326>
3. East Coast Fever. In: GALVmed [Internet]. [cited 12 Feb 2021]. Available: <https://www.galvmed.org/livestock-and-diseases/livestock-diseases/east-coast-fever/>
4. Minjauw B, McLeod A. Tick-borne diseases and poverty. The impact of ticks and tickborne diseases on the livelihood of small-scale and marginal livestock owners in India and eastern and southern Africa. 2003 [cited 1 Feb 2019]. Available: <http://agris.fao.org/agris-search/search.do?recordID=GB2012100456>
5. Cumming GS, Vuuren DPV. Will climate change affect ectoparasite species ranges? *Glob Ecol Biogeogr*. 2006;15: 486–497. doi:<https://doi.org/10.1111/j.1466-822X.2006.00241.x>
6. Neitz WO. Theileriosis, gonderioses and cytauxzoonoses: a review. *Onderstepoort J Vet Res*. 1957;27. Available: <https://repository.up.ac.za/bitstream/handle/2263/58628/19neitz1957a.pdf?sequence=1>
7. Epstein H. The origin of the domestic animals of Africa. Africana Publishing Corporation; 1971. Available: <https://cgospace.cgiar.org/handle/10568/70619>
8. Ndungu SG, Brown CGD, Dolan TT. In vivo comparison of susceptibility between Bos indicus and Bos taurus cattle types to Theileria parva infection. *Onderstepoort J Vet Res*. 2005;72: 13–22.
9. Barnett SF. Theileriosis control. *Bull Epizoot Afr*. 1957;5: 343–357.
10. Irvin AD, Cunningham MP, Young AS, editors. *Advances in the Control of Theileriosis: Proceedings of an International Conference held at the International Laboratory for Research on Animal Diseases in Nairobi, 9–13th February, 1981*. Springer Netherlands; 1981. Available: <https://www.springer.com/gb/book/9789024725755>
11. Sitt T, Poole EJ, Ndambuki G, Mwaura S, Njoroge T, Omondi GP, et al. Exposure of vaccinated and naive cattle to natural challenge from buffalo-derived Theileria parva. *Int J Parasitol Parasites Wildl*. 2015;4: 244–251. doi:10.1016/j.ijppaw.2015.04.006
12. Sepahi A, Kraus A, Casadei E, Johnston CA, Galindo-Villegas J, Kelly C, et al. Olfactory sensory neurons mediate ultrarapid antiviral immune responses in a TrkA-dependent manner. *Proc Natl Acad Sci*. 2019;116: 12428–12436. doi:10.1073/pnas.1900083116
13. Küenzi P, Schneider P, Dobbelaere DAE. Theileria parva-transformed T cells show enhanced resistance to Fas/Fas ligand-induced apoptosis. *J Immunol Baltim Md* 1950. 2003;171: 1224–1231.

14. de Clare Bronsvoort BM, Thumbi SM, Poole EJ, Kiara H, Auguet OT, Handel IG, et al. Design and descriptive epidemiology of the Infectious Diseases of East African Livestock (IDEAL) project, a longitudinal calf cohort study in western Kenya. *BMC Vet Res.* 2013;9: 171. doi:10.1186/1746-6148-9-171
15. Callaby R, Jennings A, Mwangi ST, Mbole-Kariuki M, Van Wyk I, Kiara H, et al. Reflections on IDEAL: What we have learnt from a unique calf cohort study. *Prev Vet Med.* 2020;181: 105062. doi:10.1016/j.prevetmed.2020.105062
16. Latre de Late P, Cook EAJ, Wragg D, Poole EJ, Ndambuki G, Makau MC, et al. Inherited resistance in cattle to the apicomplexan protozoan *Theileria parva* is associated with decreased proliferation of parasite-infected lymphocytes. *bioRxiv.* 2021.
17. Morrison WI, MacHugh ND, Lalor PA. Pathogenicity of *Theileria parva* is influenced by the host cell type infected by the parasite. *Infect Immun.* 1996;64: 557–562. doi:10.1128/iai.64.2.557-562.1996
18. Dutta P, Talenti A, Young R, Jayaraman S, Callaby R, Jadhav SK, et al. Whole genome analysis of water buffalo and global cattle breeds highlights convergent signatures of domestication. *Nat Commun.* 2020;11: 4739. doi:10.1038/s41467-020-18550-1
19. Katende J, Morzaria S, Toye P, Skilton R, Nene V, Nkonge C, et al. An enzyme-linked immunosorbent assay for detection of *Theileria parva* antibodies in cattle using a recombinant polymorphic immunodominant molecule. *Parasitol Res.* 1998;84: 408–416. doi:10.1007/s004360050419
20. Odongo DO, Sunter JD, Kiara HK, Skilton RA, Bishop RP. A nested PCR assay exhibits enhanced sensitivity for detection of *Theileria parva* infections in bovine blood samples from carrier animals. *Parasitol Res.* 2009;106: 357. doi:10.1007/s00436-009-1670-z
21. Weber F, Knapp G, Ickstadt K, Kundt G, Glass Ä. Zero-cell corrections in random-effects meta-analyses. *Res Synth Methods.* 2020;11: 913–919. doi:10.1002/jrsm.1460
22. R Development Core Team. R: A Language and Environment for Statistical Computing. 2011;1: 409. doi:10.1007/978-3-540-74686-7
23. Li H. Aligning sequence reads, clone sequences and assembly contigs with BWA-MEM. *ArXiv13033997 Q-Bio.* 2013 [cited 6 Jan 2014]. Available: <http://arxiv.org/abs/1303.3997>
24. McKenna A, Hanna M, Banks E, Sivachenko A, Cibulskis K, Kernytsky A, et al. The Genome Analysis Toolkit: A MapReduce framework for analyzing next-generation DNA sequencing data. *Genome Res.* 2010;20: 1297–1303. doi:10.1101/gr.107524.110
25. DePristo MA, Banks E, Poplin R, Garimella KV, Maguire JR, Hartl C, et al. A framework for variation discovery and genotyping using next-generation DNA sequencing data. *Nat Genet.* 2011;43: 491–498. doi:10.1038/ng.806
26. Poplin R, Ruano-Rubio V, DePristo MA, Fennell TJ, Carneiro MO, Auwera GAV der, et al. Scaling accurate genetic variant discovery to tens of thousands of samples. *bioRxiv.* 2018; 201178. doi:10.1101/201178

27. Auwera GAV der, Carneiro MO, Hartl C, Poplin R, Angel G del, Levy-Moonshine A, et al. From FastQ Data to High-Confidence Variant Calls: The Genome Analysis Toolkit Best Practices Pipeline. *Curr Protoc Bioinforma.* 2013;43: 11.10.1-11.10.33. doi:10.1002/0471250953.bi1110s43
28. Chang CC, Chow CC, Tellier LC, Vattikuti S, Purcell SM, Lee JJ. Second-generation PLINK: rising to the challenge of larger and richer datasets. *GigaScience.* 2015;4. doi:10.1186/s13742-015-0047-8
29. Li H. A statistical framework for SNP calling, mutation discovery, association mapping and population genetic parameter estimation from sequencing data. *Bioinforma Oxf Engl.* 2011;27: 2987–2993. doi:10.1093/bioinformatics/btr509
30. Danecek P, Auton A, Abecasis G, Albers CA, Banks E, DePristo MA, et al. The variant call format and VCFtools. *Bioinforma Oxf Engl.* 2011;27: 2156–2158. doi:10.1093/bioinformatics/btr330
31. Manichaikul A, Mychaleckyj JC, Rich SS, Daly K, Sale M, Chen W-M. Robust relationship inference in genome-wide association studies. *Bioinforma Oxf Engl.* 2010;26: 2867–2873. doi:10.1093/bioinformatics/btq559
32. Delaneau O, Marchini J, Zagury J-F. A linear complexity phasing method for thousands of genomes. *Nat Methods.* 2012;9: 179–181. doi:10.1038/nmeth.1785
33. O’Connell J, Gurdasani D, Delaneau O, Pirastu N, Ulivi S, Cocca M, et al. A General Approach for Haplotype Phasing across the Full Spectrum of Relatedness. *PLOS Genet.* 2014;10: e1004234. doi:10.1371/journal.pgen.1004234
34. Howie BN, Donnelly P, Marchini J. A Flexible and Accurate Genotype Imputation Method for the Next Generation of Genome-Wide Association Studies. *PLOS Genet.* 2009;5: e1000529. doi:10.1371/journal.pgen.1000529
35. Hamming RW. Error detecting and error correcting codes. *Bell Syst Tech J.* 1950;29: 147–160. doi:10.1002/j.1538-7305.1950.tb00463.x
36. Dobin A, Davis CA, Schlesinger F, Drenkow J, Zaleski C, Jha S, et al. STAR: ultrafast universal RNA-seq aligner. *Bioinforma Oxf Engl.* 2013;29: 15–21. doi:10.1093/bioinformatics/bts635
37. Anders S, Pyl PT, Huber W. HTSeq—a Python framework to work with high-throughput sequencing data. *Bioinformatics.* 2015;31: 166–169. doi:10.1093/bioinformatics/btu638
38. McLaren W, Gil L, Hunt SE, Riat HS, Ritchie GRS, Thormann A, et al. The Ensembl Variant Effect Predictor. *Genome Biol.* 2016;17: 122. doi:10.1186/s13059-016-0974-4
39. Untergasser A, Nijveen H, Rao X, Bisseling T, Geurts R, Leunissen JAM. Primer3Plus, an enhanced web interface to Primer3. *Nucleic Acids Res.* 2007;35: W71–W74. doi:10.1093/nar/gkm306
40. Goddeeris BM, Morrison WI. Techniques for the generation, cloning, and characterization of bovine cytotoxic T cells specific for the protozoan *Theileria parva*. *J Tissue Cult Methods.* 1988;11: 101–110. doi:10.1007/BF01404140

531 **Supporting Information**

532 **S1 Table. Phenotypic data for animals involved in field trials**

533 **S2 Table. Daily temperature observations per animal during field trials.**

534 **S3 Table. Results of modeling to fit survival status in response to haplotype distances**

535 **S4 Table. Results of eQTL modeling**

536 **S5 Table. Results of eQTL beta comparisons to identify response eQTL**

537 **S6 Table. Variant Effect Predictor output for variants identified in the genomic interval associated**

538 **with tolerance to *Theileria parva* infection, 15:45-51 Mb**